# Chapter 6
# Ceramics: Effect of Powder and Slurry Properties on Quality

**Makio Naito**

**Abstract** Ceramics are widely used in industry. Especially, advanced ceramics are of growing importance for a large variety of industrial applications in relation to excellent features like high mechanical strength, high stability and high functional properties. Good performance results not only from details of ceramic powders but also from adequate focus on the details of the processing steps for manufacturing the ceramic products. This chapter focuses on the detrimental effect that the presence of few large particles, slurry properties and the structure and mechanical properties of granules in the green body have on the strength of the ceramic product. They have been found to initiate weak spots in ceramic products. Also, some new measurement approaches are explained that allow identification of the fracture origin.

## 6.1 Introduction

"Ceramics" originates from the Greek word "keramikos" (κεραμικός). It means 'pottery', which actually has been widely used for human life. The opportunity to utilize ceramics as advanced materials started from the beginning of the twentieth century. Ferrite was invented in the 1930s, the dielectric Barium Titanate ($BaTiO_3$) was discovered in the early 1940s, and then various kinds of ceramics have been developed after the 1950s. This means that microstructure control of ceramics can create specific functional applications including mechanical, thermal, chemical, electrical, magnetic, optical and combinations thereof.

Although ceramics have been used for many applications, still serious problems remain on reliability of mechanical strength and their forming into various shapes. As ceramics are manufactured by using powder materials, their manufacturing

M. Naito (✉)
Joining and Welding Research Institute, Osaka University, Japan
e-mail: m-naito@jwri.osaka-u.ac.jp

H.G. Merkus and G.M.H. Meesters (eds.), *Particulate Products: Tailoring Properties for Optimal Performance*, Particle Technology Series 19,
DOI 10.1007/978-3-319-00714-4_6, 

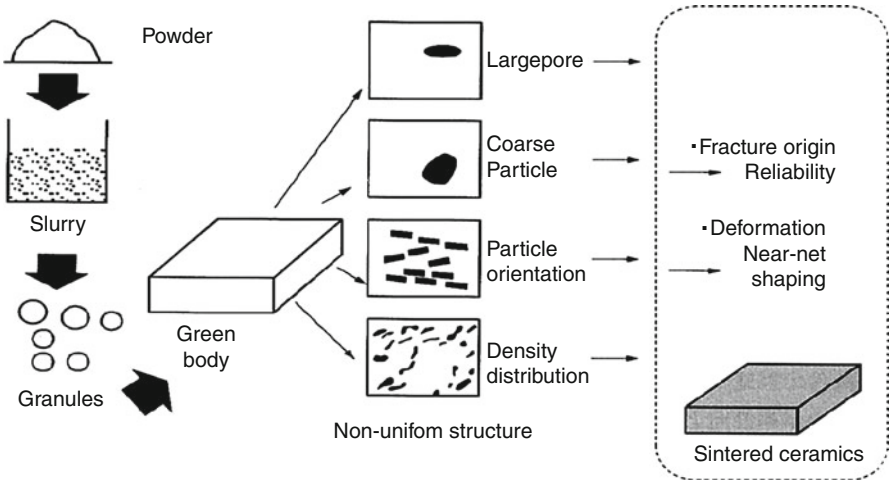


**Fig. 6.1** Powder granule compaction process to make sintered ceramics

process has a major influence on the properties of the final product. This chapter addresses various aspects that are essential for manufacture of ceramic products of high quality, viz. details of the particle size distribution (PSD) and powder process conditions. The reason is that a few coarse particles as well as improper conditions in the manufacturing process may lead to significant decrease of ceramic strength. In addition, some new measurement approaches will be described that allow identification of weak spots in ceramic bodies.

Figure 6.1 shows a typical powder granule compaction process used for manufacturing [27] sintered ceramics. The typical process steps are: bringing the dry ceramic powder into an aqueous slurry, spray-drying this slurry into granules, pressing the granules into a green body having the required shape and sintering this shape at about 1,000–1,700 °C into the ceramic product. Note that a non-uniform structure, by presence of a few large pores or coarse particles in the green compact, may become the origin of fracture [3, 4], which affects the reliability of sintered ceramics. On the other hand, optimum particle packing resulting from adequate particle orientation or powder packing density distribution in the green compact, leads to good fracture strength and final shaping. Therefore, the manufacturing process of green compact before firing is crucial for producing high quality ceramics [34].

In this chapter, the manufacturing process of silicon nitride and alumina ceramics is used to elucidate the relationship between the powder processing conditions and the fracture origin in the ceramic products, which is the most basic factor for their quality. The effect of each processing condition of powder, powder slurry, powder granule and green body on the properties of sintered ceramics is discussed. Detailed characterization of powder raw materials, powder slurry, powder granules, green body, and sintered body is found necessary to understand and control ceramic processing conditions and is essential to open the black box of ceramic manufacturing processes using raw powder materials.

## 6.2 Selection of Raw Powder Materials and Their Grinding Conditions

Raw powder material is very important in ceramics for various aspects. It is one of the most decisive factors for the quality of a product [19]. The use of proper raw material is critical for producing ceramics of high quality at minimal costs. Raw powder materials of high quality are available in the market place. Proper selection of both powders and their processing is crucial for manufacturing high quality of ceramics.

General criteria for good raw powders are shown in Table 6.1 [35]. They may vary, however, with application and the technical level of processing. For example, fine powders are desirable for many applications, at least in principle, for their low sintering temperature, the resultant fine grains after sintering and high quality of products. In practice, however, their processing is often very difficult without high skill, and the quality of ceramics made from them may be lower than that made from coarse powders, if they are inadequately processed. For advanced ceramics, how to process fine powders is critical for high quality.

In the initial phase of the ceramics processing, dry powder is dispersed in water to form a slurry in the so-called grinding or dispersion step, in e.g. ball mills. Conventionally, PSD's of these slurries are characterized by gravitational sedimentation or laser diffraction method. However, these conventional characterization tools are insufficient to detect very small amounts of non-uniform components. For example, Fig. 6.2 shows the particle size distribution of ground silicon nitride powder by wet ball milling [21]. It was measured by X-ray

**Table 6.1** Criteria for good raw ceramic powder

| | | |
|---|---|---|
| **Chemistry** | Composition | Homogeneous |
| | Impurities | None |
| | Stoichiometry | Stoichiometric |
| | Phase | Stable |
| **Particles** | Shape | Uniform and spherical for most applications |
| | Size range | 0.1–30 μm (depending on application) |

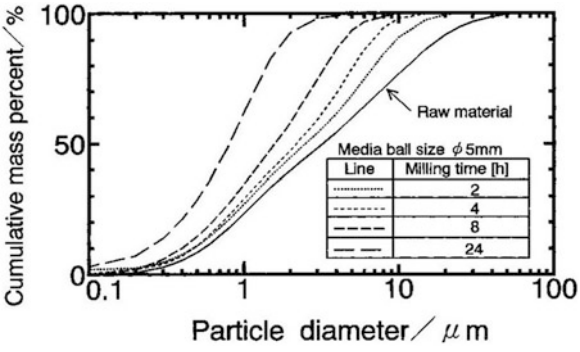


**Fig. 6.2** PSD from X-ray sedimentation of $Si_3N_4$ powder ground with 5 mm media balls, at different milling times

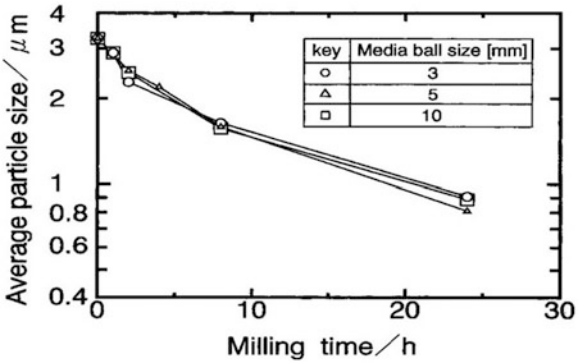


**Fig. 6.3** Relationships between average particle size of ground powder and milling time

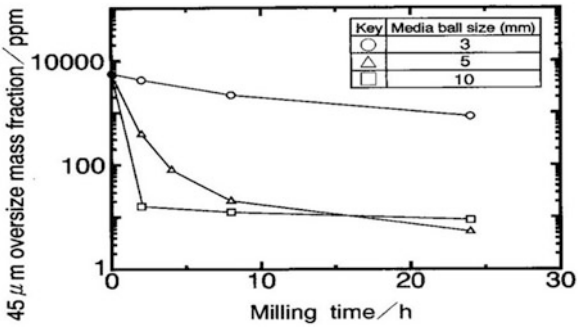


**Fig. 6.4** Change of 45 μm oversize mass fraction of ground powder with milling time while using different media ball sizes, measured by wet sieving

sedimentation method [8, 22]. The obtained PSD indicates that the ground powder has no particles coarser than 45 μm. Furthermore, Fig. 6.3 shows the relationships between average particle size of ground powder and ball-milling time [21]. It shows that average particle size usually used for characterizing ceramic powders decreases with the milling time; and, media ball size has no effect in this case. However, the situation was quite different when using wet sieve analysis to examine the 45 μm oversize mass fraction of the ground powder with ball-milling time [21], as can be seen in Fig. 6.4. Different from Fig. 6.2, it shows that coarse particles larger than 45 μm are apparently contained in the ground powder, at a concentration level of about 10–1,000 ppm or about 30–3,000 particles per gram. Media ball size has effect on the change of its mass fraction in the ground powder with milling time. The 10 mm sized media ball is the most effective to grind coarse particles. The results indicate that the wet sieve analysis is a more reliable method to measure a few large particles in the ground powder. Apparently, these small amounts of $45^{+}$ μm $Si_3N_4$ particles cannot be detected by the sedimentation method used. There may be two reasons. One is that the sedimentation of these particles in water is very fast (within few seconds), so that they have left the detection zone almost right after starting the analysis. The second reason may be that 10–1,000 ppm of coarse particles is below the lower limit of the concentration measurement of this method.

From Fig. 6.4, we can identify the optimum grinding conditions to reach a minimum amount of coarse particles. As a result, a method to measure coarse particles in advanced ceramic powder was developed [7, 28], which has been filed as an international standard in advanced ceramics [18]. By relating the coarse particle information of raw powder or powder slurry to that of sintered ceramics, we can easily understand how small amounts of coarse particles lower the reliability of sintered ceramics. An example will be explained in Sect. 6.4.

## 6.3 Effect of Slurry Preparation Conditions on Powder Granule Properties

Slurry preparation conditions can directly affect the powder granule properties made by spray drying and may lead to non-uniform structure of green compact [5]. Figure 6.5 shows the fabrication process of silicon nitride ceramics by powder granule compaction [24].

Commercially available silicon nitride, alumina, and yttrium oxide powders were used as the starting materials. Average particle size of each powder measured by gravitational X-ray sedimentation was 0.44, 0.33, and 0.29 μm, respectively. Silicon nitride powder (270 g) was mixed with alumina (15 g) and yttrium oxide (15 g) by ball-milling with distilled and deionized water (155 g) for 24 h. Dispersant was not added because the pH of the slurry moved to the basic region (up to 10.5) during mixing, at which silicon nitride is deflocculated electrostatically, due to the reaction of silicon nitride and water. After passing through a sieve (32 μm) to remove undesired large agglomerates or coarse particles, the slurry was divided into two parts. One part was kept in the well-dispersed state at pH 10.5. Apparent viscosity of the slurry was measured with a viscometer to be 300 mPa.s at a shear rate of 60 $min^{-1}$. In the other part, the pH was lowered to 9.4, through slowly adding a dilute aqueous $HNO_3$ solution while continuous stirring at room temperature. Agglomeration occurred as indicated by the strong increase of the apparent viscosity to 6,500 mPa·s. Both slurries were then spray-dried to form powder granules.

Figure 6.6 shows micrographs of the granules prepared from the well-dispersed slurry and the flocculated slurry [24]. One picture was obtained with SEM, the other two were observed with optical microscope, while using an immersion liquid of about the same refractive index as the particles, which makes the particles transparent [36, 37]. In this latter method, the internal structure of the granules is clearly visible.

Most granules prepared from the well-dispersed slurry have distorted spherical shapes and contain dimples, which are visible in the SEM picture and as light spots in the micrograph taken in the optical transmission mode, as shown in Fig. 6.6a, b. In contrast, the granules prepared from flocculated slurry were essentially spherical and had no dimples, as shown in Fig. 6.6c. It indicates

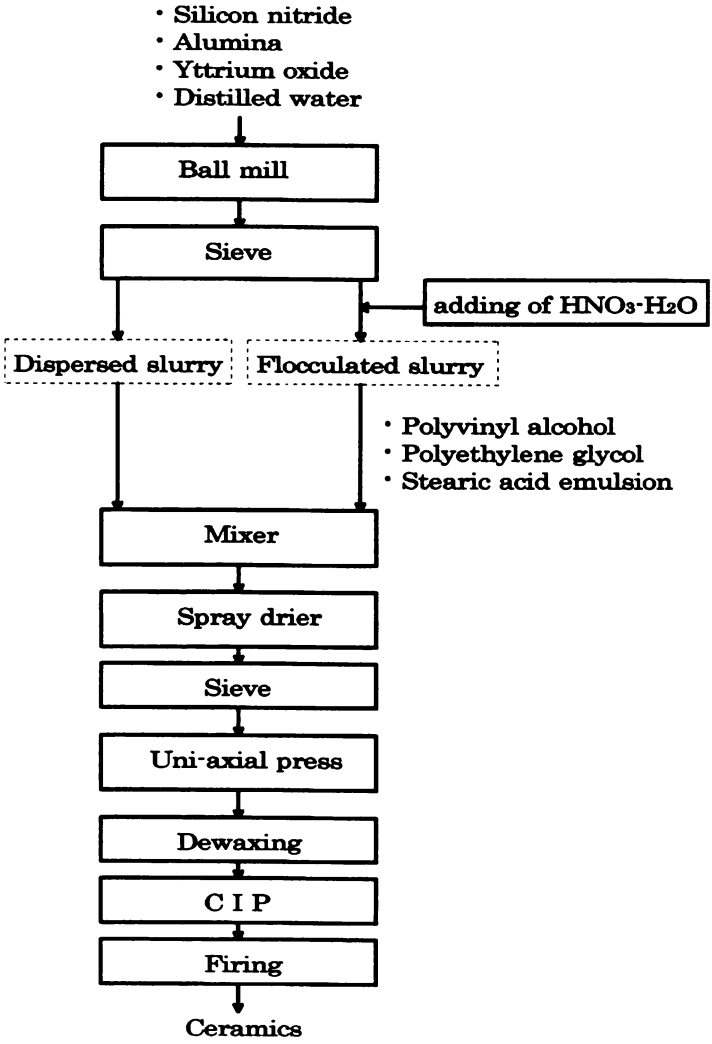


**Fig. 6.5** Fabrication process of silicon nitride ceramics

that better characterization tools are necessary to observe possible non-uniform structure in granules.

Figure 6.7 shows the Weibull distribution curves of the flexural strength of the sintered $Si_3N_4$ bodies. (see Annex 6A) [24]. Average strength[1] of sintered body fabricated from flocculated slurry (717 MPa) was obviously higher than that from well-dispersed slurry (607 MPa), although the calculated Weibull moduli were high for both of them. The fractographical analysis for the fractured specimen

[1] In this chapter, average strength of sintered body means the arithmetic average of measured mechanical strength values.

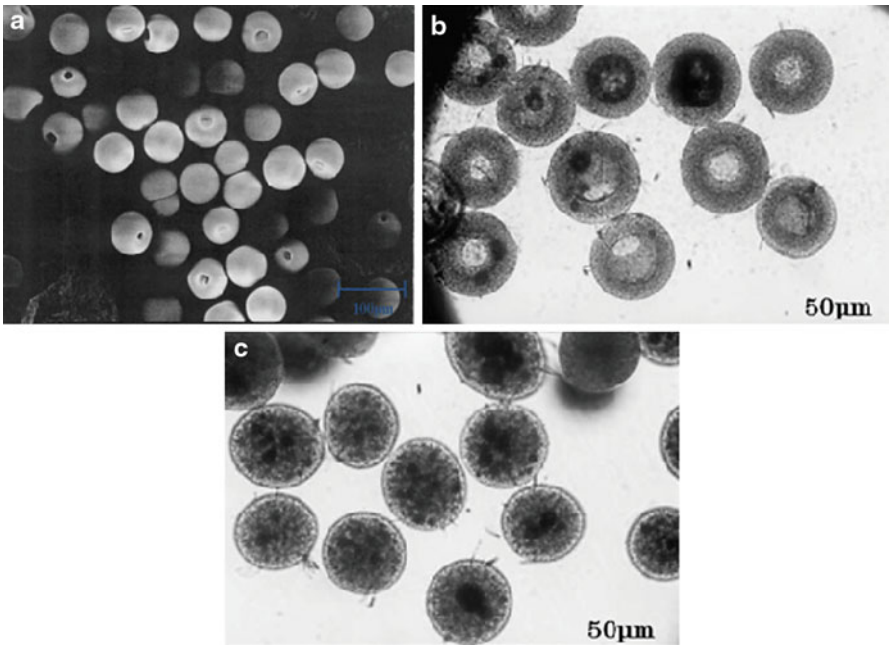


**Fig. 6.6** Morphology of $Si_3N_4$ granules observed by SEM and liquid immersion method; (**a**) SEM picture of granules prepared from well-dispersed slurry, (**b**) liquid immersion method, granules from well-dispersed slurry, (**c**) liquid immersion method, granules from flocculated slurry

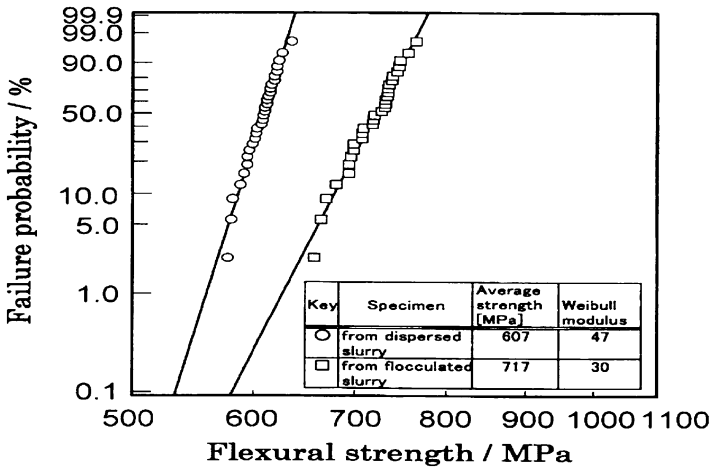


**Fig. 6.7** Weibull distributions of the fracture strength measured for sintered $Si_3N_4$ specimens

clearly indicates that large pore defects were responsible for fracture [24]. Such larger pore defects in the ceramics originated from the shape and the internal structure of particles in the granules. In this case, large pores starting at the centers of granules originated from dimples through powder packing during

**Table 6.2** Slurry preparation conditions and properties of the sintered alumina ceramics

| No. | pH | Dispersant amount [mass%] | Viscosity [mPa · s] | Density [kg/m$^3$] | Fracture toughness [MPam$^{1/2}$] |
|---|---|---|---|---|---|
| #1 | 10 | 0.2 | 43 | $3.91 \times 10^3$ | 3.7 |
| #2 | 9.1 | 0.5 | 22 | $3.94 \times 10^3$ | 3.8 |
| #3 | 8.1 | 2.0 | 54 | $3.89 \times 10^3$ | 3.8 |

compaction and those at the boundaries caused by incomplete adhesion between granules affect the fracture strength of ceramics. In the experiment, large pore size was apparently larger in the thinned specimen of the sintered ceramics made by well-dispersed slurry [10, 29].

Although the structure of powder granules is similar, the fracture strength of the sintered bodies may still be affected by other aspects of the slurry preparation conditions [1]. Alumina powder (AL160-SG4, Showadenko, Japan, average particle size: 0.46 μm) was mixed with 0.2 %, 0.5 %, 2.0 % w/w of polymer dispersant (ammonium polyacrylate, CELUNA-D305, Chukyoyushi, Japan) and distilled and deionized water for 24 h by ball milling. The solid concentration of the slurry was 35 % v/v. Table 6.2 indicates the preparation conditions of three slurries and their difference in apparent viscosity [1]. The pH of slurry with 0.2 % w/w dispersant was increased to 10 by adding dilute $NH_4OH$ solution, which decreased its viscosity to 43 mPa·s. The slurries were spray-dried for granulation. The granules were uni-axially pressed at 9.8 MPa, and then isostatically pressed at 176 MPa. The green compacts were sintered at 1550 °C for 2 h in air. As indicated in Table 6.2, the three slurries showed low apparent viscosity. Their granules had distorted spherical shapes and contained dimples, which were clearly visible in the micrograph taken under the optical transmission mode, as shown in Fig. 6.6b. Also, no big difference was observed in size distribution of granules made from the three slurry preparing conditions, and their average sizes were all about 60 μm.

Table 6.2 presents the density and fracture toughness of the specimens. The values are almost the same for these ceramics. Figure 6.8 shows the strength distribution of the alumina ceramics [1]. A significant variation of strength associated with the slurry preparation condition was noted. The average strength is 486, 430 and 363 MPa, respectively, for specimens made from the three slurry preparing conditions.

Figure 6.9 shows a comparison of the compressive strength of the granules prepared from the three different slurries [1]. The strength of granules was measured with a micro compression test machine (MCTM-500, Shimadzu Co., Japan) and the compressive strength was calculated by applying the model proposed for the fracture of spherical rock particle [9, 23].

Figure 6.10 shows the transmission optical micrograph of the thinned ceramics specimens without any immersion liquid [1]. The dark features are large pores in the structures. Clearly, the present ceramics have defects at the center and boundaries of granules. They are developed from the irregularities of packing structure of powder particles in green compact. The pore shape was similar for

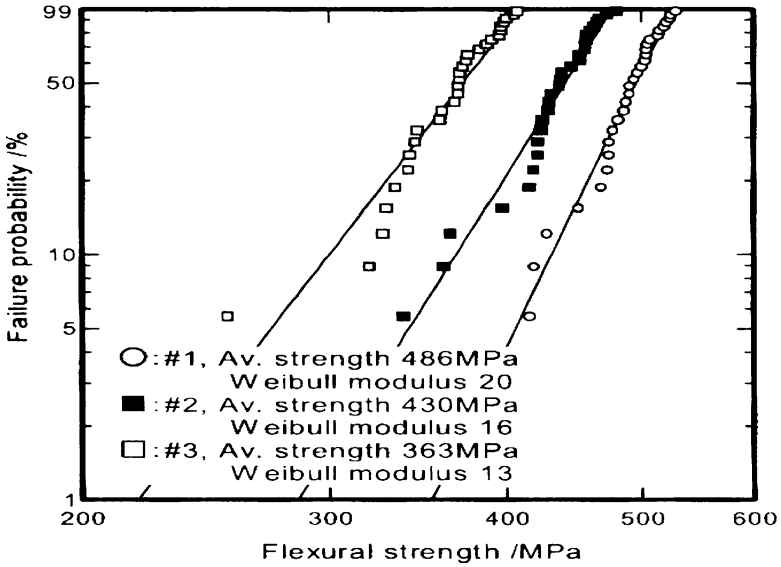


**Fig. 6.8** Strength distribution of the alumina ceramics

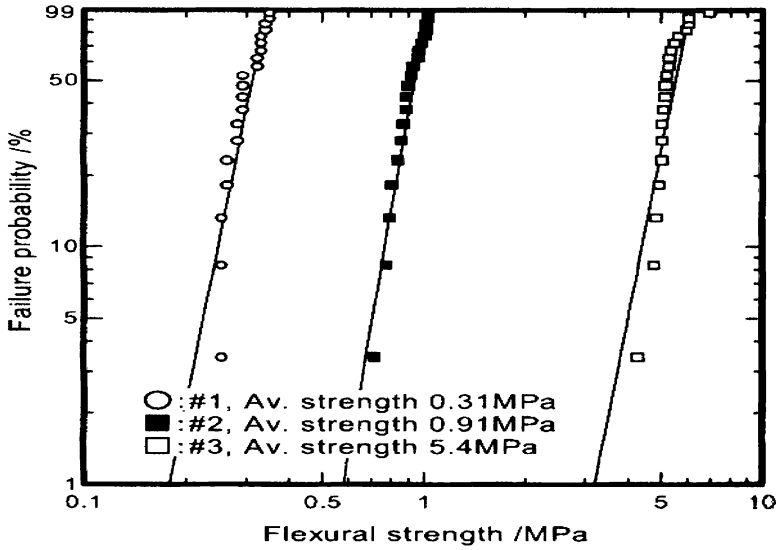


**Fig. 6.9** Compressive strength distribution of alumina granules associated with different slurry preparation conditions

the three specimens, except for the size of the pores associated with the slurry preparing condition. The relation between the pore number density versus the pore size of the sintered specimens made from the three slurries was measured [1]. The pore number density was defined as the number of pore per unit volume of

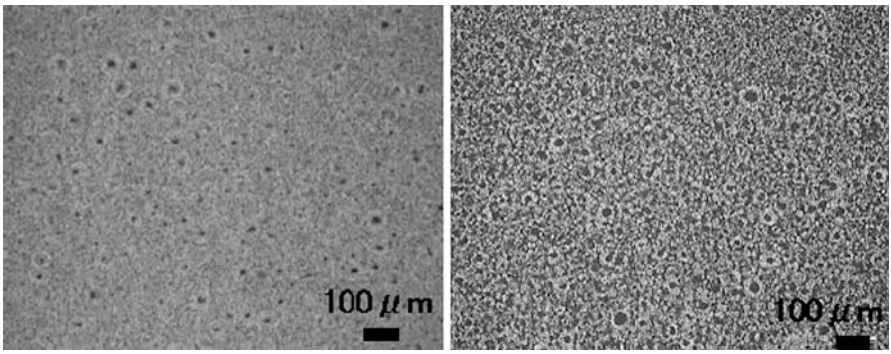


**Fig. 6.10** Microstructures of alumina ceramics examined with optical transmission technique; *left*: specimen made from the slurry prepared with #1 condition *right*: specimen made from the slurry prepared with #3 condition

specimen per unit size interval. The effective volume of specimens under the analysis was about 0.5 $mm^3$. In this study, relatively large pores were analyzed. Pores were assumed to have a spherical shape and their sizes were represented by the equivalent diameter.

According to the fracture mechanics, the strength of ceramics $\sigma$, can be related to the size of fracture origin, $c$, by the following equation:

$$K_{IC} = \sigma Y c^{1/2} \tag{6.1}$$

Where $K_{IC}$ is the fracture toughness and $Y$ is a shape factor.

As expected from the equation, fracture strength of ceramics will depend on the size of fracture origin, provided that the fracture toughness and the shape factor are the same. Focusing on large pores, the size as shown in Fig. 6.10 (right) is 1.29 times larger than that in the specimen shown in Fig. 6.10 (left). Provided the shape factor is the same, the strength of the sintered sample made from the slurry of pH 10 is estimated 1.34 times higher than that made from the slurry of pH 8.1. This estimate is in good agreement with the measured average strength as shown in Fig. 6.8.

The change of the large pore size can be ascribed to the difference in the granule strength as shown in Fig. 6.9. In compaction of harder granules, less deformation can occur at a certain compaction pressure and this leaves larger pores in compacts. The size of large pore increases with the granule strength, which was strongly affected by the amounts of dispersant in slurry as shown in Fig. 6.9.

The granule strength is influenced by various factors, such as the powder packing structure as well as the amount and distribution of dispersant in granules [20]. In this study, the difference of the granule strength can be ascribed to the latter factor dominantly, since the granule structure was almost similar. Note that the amounts of dispersant added, 0.2, 0.5 and 2.0 % w/w, are insufficient, a little excess and excess, resp., for covering the powder surfaces, based on the relation between

the amounts of dispersant and the slurry viscosity, respectively. With excessive dispersant, the non-adsorbed dispersant introduces free polymers in the slurry, which increases the apparent viscosity. In spray-drying, the free polymers form solid bridges between powder particles, increasing the granule strength considerably. Clearly, polymeric additives have critical effects on the cohesive force between particles and thus on the powder compaction process.

## 6.4 Effect of Coarse Particles in Powder Slurry on the Quality of Ceramics

Control of particle size distribution of ceramic powder is also important in slurry preparation. Powder is dispersed in water using mechanical method such as ball milling. A fundamental study was conducted to understand the effect of coarse particles on the fracture strength of ceramics. The specimens were prepared through the procedure as shown in Fig. 6.11 [13].

Low-soda alumina powder (AL-160SG-4, Showa Denko K.K., Japan) was used as raw material. The nominal average particle size was 0.5 μm. The powder was placed in alumina ball mill container (SSA-999, Nikkato, Japan, volume 2000 ml) with 2 kg of alumina balls (SSA-999, Nikkato; diameter 5 mm), and 400 g of aqueous solution (2 % w/w) of dispersant of polyacrylic acid type (CERUNA D-305, Chukyo Yushi, Japan) and mixed for 24 h to make a slurry with 50 % v/v solid content. The slurry was passed through a mesh (2 mm opening) to separate the balls. Weighed slurry was placed in a container and stirred continuously while a small amount of coarse particles (0.01–0.1 % w/w) was added. These coarse particles were prepared from the unground raw material used in the production of the present fine alumina powder. They were classified into three fractions by sieving before being used. A single fraction of coarse particles was added to individual slurry; therefore, three kinds of slurries with coarse particles were prepared. Each slurry was kept stirring for 2 h after the coarse particles were added. Finally each slurry, was cast in gypsum molds (100 × 100 × 9 mm) to prepare green compacts. After drying, the compact was heated at 1,550 °C for 2 h in an electric furnace to sinter the model ceramics [13].

At high magnification by SEM, it was found that the platelet-shape particles formed aggregates of porous structure with the size of 10–20 μm [13]. At lower magnification, these aggregates formed the coarse aggregates in large scale. In this experiment, such coarse aggregates are referred to as coarse particles. Table 6.3 shows the measured densities of green compact and ceramics [13]. The densities were approximately the same for all green bodies and ceramics. Clearly, addition of a small amount of coarse particles has no effect on the densities of ceramics.

Figure 6.12 shows the Weibull plots and the fracture toughness for all specimens [13]. The specimen strength decreased with increasing size of coarse particles added. The Weibull moduli were similar and over 20 for all specimens. All

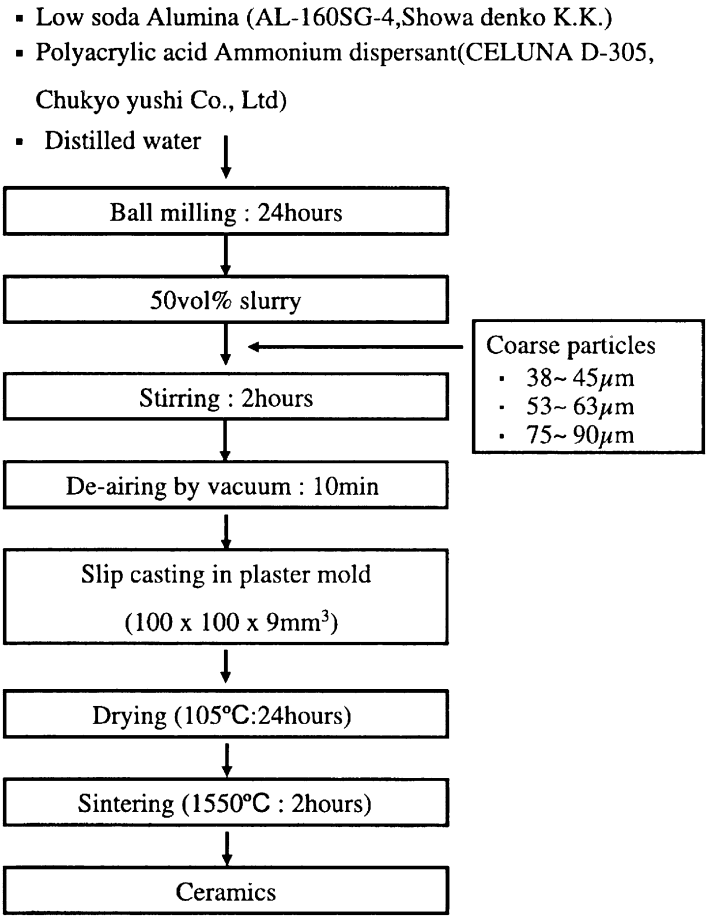


**Fig. 6.11** Fabrication process of alumina ceramics

**Table 6.3** Densities of green and sintered alumina bodies

| | Density/$10^3$ kg $m^{-3}$ | |
|---|---|---|
| Coarse particles size, sieve apertures/μm | Green body | Sintered body |
| 38–45 | 2.31 | 3.95 |
| 53–63 | 2.32 | 3.95 |
| 75–90 | 2.31 | 3.96 |

ceramics basically have the same fracture toughness. Figure 6.13 shows SEM micrographs of representative fracture origins found in this study [13]. The specimen contains coarse particles of the size range 75–90 μm. The fracture origin was noted in the specimen of the lowest strength (370 MPa) as seen in Fig. 6.13 (left); Fig. 6.13 (right) shows the origin in the specimen at having a strength of 406 MPa.

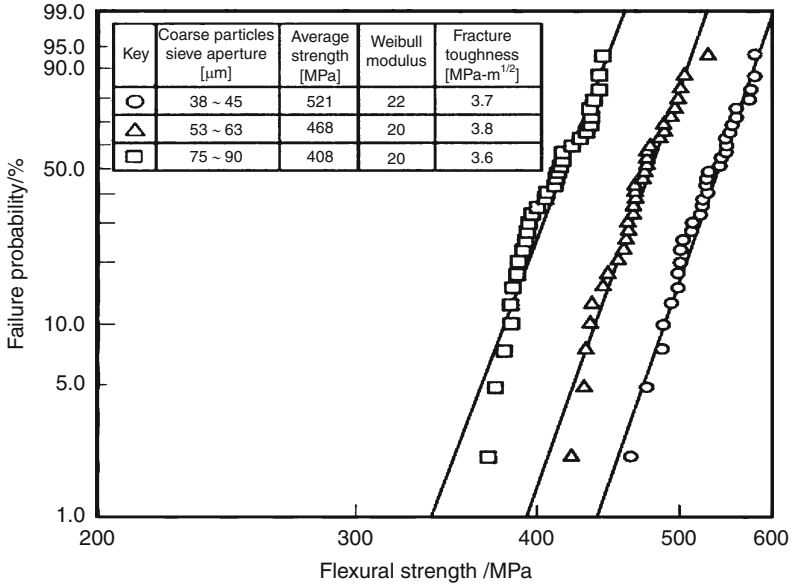


**Fig. 6.12** Mechanical properties of sintered alumina bodies

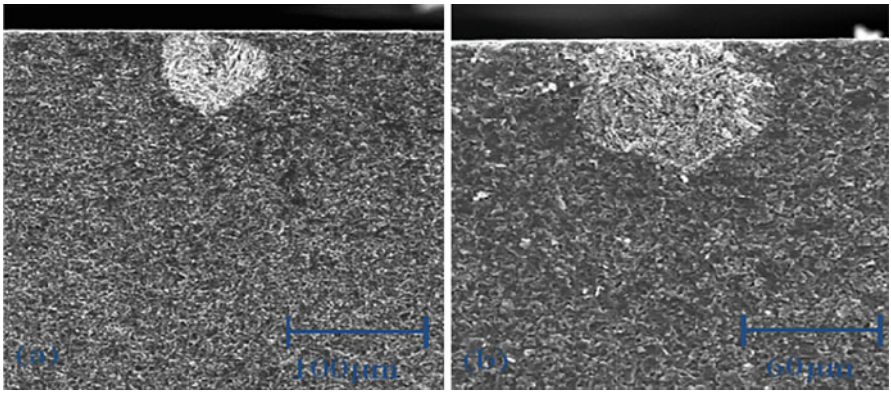


**Fig. 6.13** Examples of fracture origins in alumina ceramics containing; 75 ~ 90 μm coarse particles. (*left*) 370 MPa, (*right*) 406 MPa

In both cases, fracture originated at the coarse particles. Lower strength was observed for the specimen containing larger coarse particles.

Figure 6.14 shows IR photomicrographs [38] for the internal structures of ceramics containing coarse particles of various sizes [13]. In the micrographs, the dark spots show coarse particles. The size of coarse particles in the ceramic matrix increased with increasing size of coarse particles added. Again, the sizes of coarse particles are the same as those added in the preparation of specimens [13]. Actually,

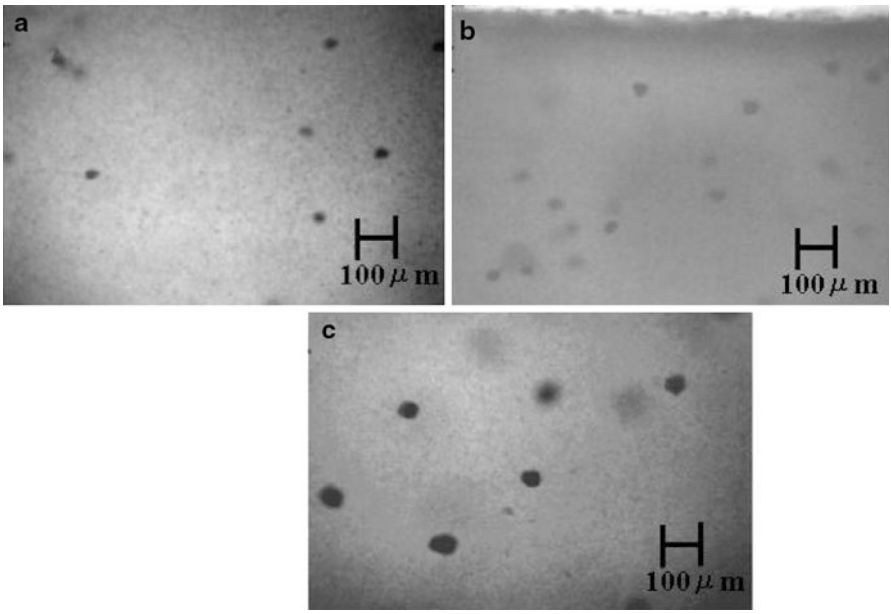


**Fig. 6.14** Mid-infrared micrographs of sintered bodies with coarse particles of (**a**) 38 ~ 45 μm, (**b**) 53 ~ 63 μm, (**c**) 75 ~ 90 μm

the estimated values of strength obtained by linear fracture mechanics, assuming that the fracture was always initiated at the coarse particles in the matrix, agrees very well with the measured strength [13]. It means that small amounts of coarse particles decrease the strength of ceramics. Therefore, careful prevention of presence of coarse particles is crucial to maximize the strength of high quality ceramics [14].

## 6.5 Influence of the Compaction Process on the Quality of Ceramics

Compaction process including uniaxial press and Cold Isostatic Pressing (CIP) affects the properties of green body through powder granule compaction route and thus affects the reliability of sintered ceramics. In this Section, the origin of the strength variation associated with the change of CIP condition in a powder granule compaction processing of silicon nitride ceramics is firstly explained.

The manufacturing process for the experiments is presented in Fig. 6.5. In this experiment, dispersed slurry was applied to prepare powder granule, therefore, the obtained granules have distorted spherical shapes and contain dimples, which are also clearly visible in the micrograph taken in the optical transmission mode, as shown in Fig. 6.6b. All granules were 150 μm-sieved to remove large aggregates and foreign objects. The average granule size was 55 μm. Then, they were

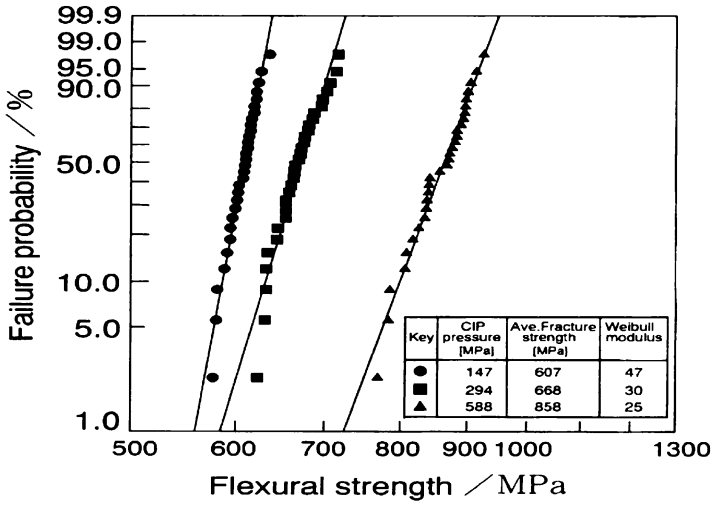


**Fig. 6.15** Influence of CIP condition on strength distribution of silicon nitride ceramics

uni-axially pressed in a square die (60 × 50 mm) at an applied pressure of 19.6 MPa. After dewaxing at 530 °C for 15 h in air, the mold-pressed green bodies were cold isostatically pressed (CIP) at 147, 294 and 588 MPa. The green bodies were embedded in boron nitride powders with a silicon nitride container and sintered at 1700 °C for 3 h under nitrogen atmosphere.

Figure 6.15 shows the strength distribution of the ceramics sintered from the three green bodies [2]. The average strength increases with increasing CIP. Their values are 607, 668 and 858 MPa for specimens sintered from green bodies with CIP pressures of 147, 294 and 588 MPa, respectively. The Weibull modulus exceeding 20 was noted for all specimens. The corresponding densities and the values of fracture toughness were essentially the same.

The direct observation methods were successfully applied to examine the origin of strength variation. All relevant structures in the processing, such as the powder granule, their green bodies and sintered bodies were examined by the transmission mode of an optical microscope.

These examinations directly showed the relation between the CIP conditions and the formation of large defects. With increasing CIP pressure, the granules were deformed, packed more tightly and isostatically. The large pores originated from the boundaries of granules even in the green body prepared at high CIP (588 MPa). The variation of fracture strength was quantitatively correlated to the internal large pore size and concentration in sintered bodies [2]. The same tendency was also reported for the sintered ceramics made by flocculated slurry [26] and the manufacturing process of AlN ceramics [6].

Granules often retain their shape in green bodies during consolidation. Intergranular pores and flaws caused by the incomplete deformation and fracture of granules are usually large and often exert a serious influence on the properties of

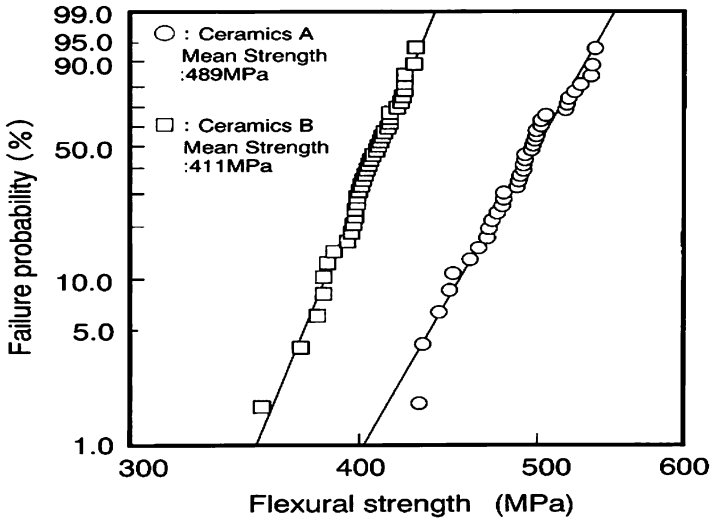


**Fig. 6.16** Weibull distribution curves of flexural strength measured for sintered specimens A and B

sintered ceramics. It means that the control of granule properties for high quality green body is key issue for the fabrication of highly reliable ceramics [11, 25, 30, 31]. To examine the effect, the granule strength was changed. In this experiment, alumina granules were prepared by spray-drying, and divided into two groups. One group (granule A) was heat-treated at 500 °C for 5 h to remove added binders. The other group (granule B) was used for testing without prior treatment [33].

Figure 6.16 shows the Weibull distribution curves of flexural strength measured for sintered samples in both groups [33]. The variations shown in fracture strength indicate the marked influence of heat treatment of the granules on the properties of the sintered bodies. The flexural strength of the sintered body A (average 489 MPa) was clearly higher than that of the sintered body B (411 MPa). The Weibull modulus was high for both samples, suggesting that the fracture origins were uniformly large.

The hard and brittle characteristics of the heat-treated granules contributed to achieving a uniform packing structure in the green body, because the pores between granules were efficiently filled with primary powder particles caused by fracture of the granules. On the other hand, the 'as-sprayed' granules preserved more clear interfaces between granules and internal pores in the green compacts, resulting in the development of large pores, and thus, a decrease in fracture strength for the sintered body [12, 33].

The above results suggest that the alteration of CIP and de-waxing procedures affects the pore structure and the fracture strength of sintered ceramics. To examine the effect, the alumina powder granules were uni-axially mold pressed into compacts at 10 MPa with a metal mold. The compacts were then divided into two groups. One was CIP-ed subsequently followed, after mold pressing, and de-waxed

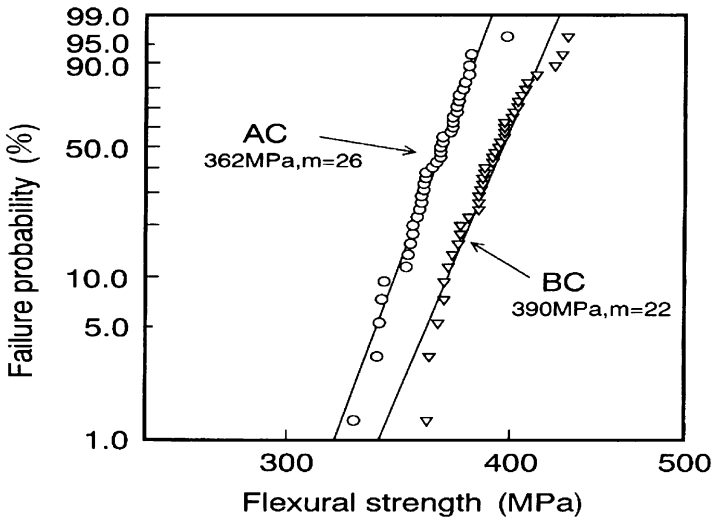


**Fig. 6.17** Weibull distributions of the flexural strength measured for the specimens made through AC and BC processes

by heat-treating at 500 °C for 5 h in the electric furnace (referred to as AC). The other was first de-waxed at 500 °C, then CIP-ed for further compaction (referred to as BC). CIP-ing was carried out at 176 MPa for green bodies in both groups and sintered at 1590 °C for 2 h in the electric furnace [32].

Figure 6.17 shows the Weibull distributions of the flexural strength measured for the specimens in both groups [32]. Flexural strength of the BC specimens was clearly higher than that of AC. Weibull modulus was high for both groups, suggesting that the size of fracture origins was rather uniformly large. De-waxing before CIP with the heat-treatment of powder compacts was effective to make the pore defect size in green and sintered bodies small and to improve the fracture strength of sintered bodies. Reduction of pore size in green compact was ascribed to the promotion of rather uniform powder packing for heat-treated and de-waxed granules. This was because the hard and brittle characteristics of the heat-treated granules contributed to achieving a uniform packing structure in the green body [33].

## 6.6 Conclusions

In this chapter, the effect of powder processing conditions on the quality of ceramics was clarified. Manufacturing processes of silicon nitride ceramics and alumina ceramics were utilized to explain the relationship between ceramics processing conditions and its major fracture origin. Powder slurry preparation conditions were found to potentially create the large pores in powder granules,

green body and sintered ceramics. These phenomena can be investigated by using new characterization tools such as the liquid immersion method and the microscopic technique observing thinned ceramics specimen under the transmission mode. Also, very small amounts of coarse particles contained in the powder slurry are weakening the strength of ceramics. This has been found by using wet sieve analysis and the observation technique with thin ceramic specimen. As a result, it is believed that major fracture origin is caused by the large pores and coarse particles, which are generated in the manufacturing steps of ceramics, such as powder slurry preparation, spray drying, and shaping process of green bodies. By making use of these characterization tools, effective processing conditions to eliminate the large pores and coarse particles can be identified for producing high quality ceramics.

## 6.7 Definitions, Abbreviations and Symbols

| | |
|---|---|
| Average strength | Arithmetic average of measured mechanical strength values of sintered body. |
| Flexural strength | Strength according to 4 point bending test method [15] |
| Fracture toughness | Toughness according to single edge pre-cracked beam (SEPB) method [16] |
| Weibull distribution | 2-parameter model distribution (see Annex 6A) |
| Weibull modulus | Spread parameter of Weibull function |
| AlN | Aluminium nitride |
| CIP | Cold isostatic pressing |
| HIP | Hot isostatic pressing |
| IR | Infrared |
| ISO | International Standards Organization |
| PSD | Particle size distribution |
| SEM | Scanning electron microscopy |
| $C$ | Size of fracture origin (Eq. 6.1) |
| $K_{IC}$ | Fracture toughness (Eq. 6.1) |
| $Y$ | Shape factor (Eq. 6.1) |

## Annex 6A

### *Weibull Distribution for Ceramic Strength*

The Weibull function is a continuous probability distribution function that can be used for many purposes. In materials science, it is often used to present the distribution of life times of objects. For ceramics and other construction materials

it is applied to express the results of mechanical strength measurements [17]. Under the name Rosin-Rammler distribution it is one of the 2-parameter model functions used for description of particle size distributions.

In its cumulative form, the function is:

$$F(x) = 1 - e^{-(x/\lambda)^k} \tag{6.2}$$

where:
$x$ = random variable (here mechanical strength, e.g. flexural strength)
$\lambda$ = scale or location parameter of the distribution
$k$ = shape or spread parameter of the distribution (Weibull modulus in case of strength)

The function can be linearized via:

$$-\ln(1 - F(x)) = (x/\lambda)^k \tag{6.3}$$

to:

$$\ln(-\ln(1 - \mathrm{F}(x))) = k(\ln x) - k(\ln\lambda) \tag{6.4}$$

Thus, by fitting the measured data to the model, or plotting ln(– ln(1–F($x$))) on the Y-axis against (ln$x$) on the X-axis of graph paper, the two parameters of the distribution can be easily calculated.

## References

1. Abe, H., Hotta, T., Kuroyama, T., Yasutomi, Y., Naito, M., Kamiya, H., Uematsu, K.: Variation of microstrucuture and fracture strength of alumina ceramics made from different slurry preparing condition. Ceram. Process. Sci. Ceram. Trans. **112**, 809–814 (2001); Am. Ceram. Soc
2. Abe, H., Hotta, T., Naito, M., Shinohara, N., Okumiya, M., Kamiya, H., Uematsu, K.: Origin of strength variation of silicon nitride ceramics with CIP condition in a powder compaction process. Powder Technol. **119**, 194–200 (2001)
3. Abe, H., Hotta, T., Naito, M., Shinohara, N., Uematsu, K.: Direct observation of detrimental defects in ceramics. Am. Ceram. Soc. Bull. **81**, 31–34 (2002)
4. Abe, H., Naito, M., Hotta, T., Shinohara, N., Uematsu, K.: Flaw size distribution in high-quality alumina. J. Am. Ceram. Soc. **86**, 1019–1021 (2003)
5. Abe, H., Naito, M., Hotta, T., Kamiya, H., Uematsu, K.: Pore defects related to slurry character and their relevance to strength distribution in alumina cermics. Powder Technnol. **134**, 58–64 (2003)
6. Abe, H., Sato, K., Naito, M., Nogi, K., Hotta, T., Tatami, J., Komeya, K.: Effects of granule compaction procedures on defect structure, fracture strength and thermal conductivity of AlN ceramics. Powder Technol. **159**, 155–160 (2005)
7. Cho, Y.-I., Okumiya, M., Naito, M., Rabe, T., Waesche, R., Morrell, R., Ewsuk, K.G., Hackley, V., Freiman, S., Uematsu, K.: Characterization of coarse particles contained in fine powders at very low concentrations. Ceram. Trans. **133**, 71–76 (2002). Am. Ceram. Soc

8. Hayakawa, O., Nakahira, K., Naito, M., Tsubaki, J.: Experimental analysis on sample preparation conditions for particle size measurement. Powder Technnol. **100**, 61–68 (1998)
9. Hiramatsu, Y., Oka, Y., Kiyama, H.: Rapid determination of tensile strength of rocks with irregular test pieces. Nihon kogyokai-shi (Jap.) **81**, 1024 (1965)
10. Hotta, T., Nakahira, K., Naito, M., Shinohara, N., Okumiya, M., Uematsu, K.: Origin of strength change in ceramics associated with the alteration of spray dryer. J. Mater. Res. **14**, 2974–2979 (1999)
11. Hotta, T., Nakahira, K., Naito, M., Shinohara, N., Okumiya, M., Uematsu, K.: Origin of the strength change of silicon nitride ceramics with the alteration of spray drying conditions. J. Eur. Ceram. Soc. **21**, 603–610 (2001)
12. Hotta, T., Abe, H., Fukui, T., Naito, M., Shinohara, N., Uematsu, K.: Effect of dewaxing procedures of cold isostatically pressed silicon nitiride ceramics on its microstructure and fracture strength. Adv. Powder Technol. **14**, 505–517 (2003)
13. Hotta, T., Abe, H., Naito, M., Takahashi, M., Uematsu, K., Kato, Z.: Effect of coarse particles on the strength of alumina made by slip casting. Powder Technol. **149**, 106–111 (2005)
14. ISO 13383–1.: Fine ceramics – determination of grain size distribution in ceramic powders by image analysis of photomicrographs (2012)
15. ISO 14704.: Fine ceramics – test method for flexural strength (2008)
16. ISO 15732.: Fine ceramics – test method for fracture toughness by single edge pre-cracked beam (SEPB) method (2003)
17. ISO 20501.: Fine ceramics – Weibull statistics for strength data (2003)
18. ISO 24369.: Fine ceramics – determination of coarse particles in ceramic powders by wet sieving method (2005)
19. Lange, L.L.: Powder processing science and technology for increased reliabilty. J. Am. Ceram. Soc. **72**, 3–15 (1989).
20. Naito, M., Fukuda, Y., Yoshikawa, N., Kamiya, H., Tsubaki, J.: Optimization of suspension characteristics for shaping processes. J. Eur. Ceram. Soc. **17**, 251–257 (1997)
21. Naito, M., Hotta, T., Hayakawa, O., Shinohara, N., Uematsu, K.: Ball milling conditions of a very small amount of large particles in silicon nitride powder. J. Ceram. Soc. Jpn (Jap.) **106**, 811–814 (1998)
22. Naito, M., Hayakawa, O., Nakahira, K., Mori, H., Tsubaki, J.: Effect of particle shape on the particle size distribution measured with the commercial equipment. Powder Technol. **100**, 52–60 (1998)
23. Naito, M., Nakahira, K., Hotta, T., Ito, A., Yokoyama, T., Kamiya, H.: Microscopic analysis on the consolidation process of granule beds. Powder Technol. **95**, 214–219 (1998)
24. Naito, M., Hotta, T., Abe, H., Shinohara, N., Okumiya, M., Uematsu, K.: Optical characterization of strength-limiting flaws in silicon nitride ceramics prepared with different slurry flocculation conditions. Proc. Br. Ceram. Soc. **61**, 119–132 (2000)
25. Naito, M., Hotta, T., Abe, H., Shinohara, N., Cho, Y.-I., Okumiya, M., Uematsu, K.: Relevance of the fracture strength to process-related defects in alumina ceramics. Mater. Trans. Jpn Inst. Met. **42**, 114–119 (2001)
26. Naito, M., Abe, H., Hotta, T., Shinohara, N., Uematsu, K.: Fracture strength variability of silicon nitride ceramics made by powder compaction. Ceram. Trans. **133**, 151–157 (2002). Am. Ceram. Soc
27. Naito, M., Abe, H.: The micromeritics. Funsai (Jap.) **48**, 56–62 (2004)
28. Nakahira, K., Hotta, T., Naito, M., Shinohara, N., Cho, Y.-I., Katori, S., Emoto, H., Yamada, T., Takahashi, T., Okumiya, M., Kumagai, C., Uematsu, K.: Characterization of coarse particles in alumina powders by wet sieving method. J. Eur. Ceram. Soc. **23**, 1661–1666 (2003)
29. Shinohara, N., Okumiya, M., Hotta, T., Nakahira, K., Naito, M., Uematsu, K.: Formation mechanisms of processing defects and their relevance to the strength in alumina ceramics made by powder compaction process. J. Mater. Sci. **34**, 4271–4277 (1999)

30. Shinohara, N., Okumiya, M., Hotta, T., Nakahira, K., Naito, M., Uematsu, K.: Effect of seasons on density, strength of alumina. Am. Ceram. Soc. Bull. **78**, 81–84 (1999)
31. Shinohara, N., Okumiya, M., Hotta, T., Nakahira, K., Naito, M., Uematsu, K.: Seasonal variation of microstructure and sintered strength of dry-pressed alumina. J. Am. Ceram. Soc. **82**, 3441–3446 (1999)
32. Shinohara, N., Okumiya, M., Hotta, T., Nakahira, K., Naito, M., Uematsu, K.: Variation of the microstrucuture and fracture strength of cold isostatically pressed alumina ceramics with the alteration of Dewaxing procedures. J. Eur. Ceram. Soc. **20**, 843–849 (2000)
33. Shinohara, N., Katori, S., Okumiya, M., Hotta, T., Nakahira, K., Naito, M., Cho, Y.-I., Uematsu, K.: Effect of heat treatment of alumina granules on the compaction behavior and properties of green and sintered bodies. J. Eur. Ceram. Soc. **22**, 2841–2848 (2002)
34. Shinohara, N., Ohsaka, S., Hotta, T., Abe, H., Naito, M., Uematsu, K.: Relevance of the internal structures to fracture strength of injection molded and sintered silicon nitride ceramics. Adv. Powder Technol. **16**, 425–434 (2005)
35. Somiya, S.,et al.: Handbook of Advanced Ceramics, Vol.1 Materials Science, p. 82. Elsevier/Academic Press, UK (2003)
36. Uematsu, K., Kim, J.-Y., Miyashita, M., Uchida, N., Saito, K.: Direct observation of internal structure in spray-dried alumina granules. J. Am. Ceram. Soc. **73**, 2555–2557 (1990)
37. Uematsu, K., Zhang, Y., Uchida, N., Hotta, T., Naito, M., Shinohara, N., Okumiya, M.: Structural flaw evaluation in green compacts and ceramics by an optical method – for understanding the origin of strength variation in ceramics. Key Eng. Mat. **161–163**, 145–150 (1999)
38. Uematsu, K., Uchida, N., Kato, Z., Tanaka, S., Hotta, T., Naito, M.: Infrared microscopy for examination of strucuture in spray-dried granules and compacts. J. Am. Ceram. Soc. **84**, 254–256 (2001)